




# Striatal Dopaminergic Depletion Pattern Reflects Pathological Brain Perfusion Changes in Lewy Body Diseases

Yu Iwabuchi<sup>1</sup>  · Tohru Shiga<sup>2</sup> · Masashi Kameyama<sup>1,3</sup> · Raita Miyazawa<sup>1</sup> · Morinobu Seki<sup>4</sup> · Daisuke Ito<sup>5</sup> · Hiroyuki Uchida<sup>6</sup> · Hajime Tabuchi<sup>6</sup> · Masahiro Jinzaki<sup>1</sup>

Received: 11 April 2022 / Revised: 23 May 2022 / Accepted: 3 June 2022 / Published online: 14 June 2022  
© The Author(s) 2022

## Abstract

**Purpose** In Lewy body diseases (LBD), various symptoms occur depending on the distribution of Lewy body in the brain, and the findings of brain perfusion and dopamine transporter single-photon emission computed tomography (DAT-SPECT) also change accordingly. We aimed to evaluate the correlation between brain perfusion SPECT and quantitative indices calculated from DAT-SPECT in patients with LBD.

**Procedures** We retrospectively enrolled 35 patients with LBD who underwent brain perfusion SPECT with N-isopropyl-p-[<sup>123</sup>I] iodoamphetamine and DAT-SPECT with <sup>123</sup>I-ioflupane. Mini-mental state examination (MMSE) data were also collected from 19 patients. Quantitative indices (specific binding ratio [SBR], putamen-to-caudate ratio [PCR], and caudate-to-putamen ratio [CPR]) were calculated using DAT-SPECT. These data were analysed by the statistical parametric mapping procedure.

**Results** In patients with LBD, decreased PCR index correlated with hypoperfusion in the brainstem (medulla oblongata and midbrain) (uncorrected  $p < 0.001$ ,  $k > 100$ ), while decreased CPR index correlated with hypoperfusion in the right temporoparietal cortex (family-wise error corrected  $p < 0.05$ ), right precuneus (uncorrected  $p < 0.001$ ,  $k > 100$ ), and bilateral temporal cortex (uncorrected  $p < 0.001$ ,  $k > 100$ ). However, there was no significant correlation between decreased SBR index and brain perfusion. Additionally, the MMSE score was correlated with hypoperfusion in the left temporoparietal cortex (uncorrected  $p < 0.001$ ).

**Conclusions** This study suggests that regional changes in striatal <sup>123</sup>I-ioflupane accumulation on DAT-SPECT are related to brain perfusion changes in patients with LBD.

**Key words**  $\alpha$ -synuclein ·  $\alpha$ -synucleinopathy · <sup>123</sup>I-FP-CIT · SPM · Parkinsonian syndrome · Parkinsonism

✉ Yu Iwabuchi  
iwabuchi@rad.med.keio.ac.jp

- <sup>1</sup> Department of Radiology, Keio University School of Medicine, Tokyo, Japan
- <sup>2</sup> Advanced Clinical Research Center, Fukushima Global Medical Science Center, Fukushima Medical University, Fukushima, Japan
- <sup>3</sup> Department of Diagnostic Radiology, Tokyo Metropolitan Geriatric Hospital and Institute of Gerontology, Tokyo, Japan
- <sup>4</sup> Department of Neurology, Keio University School of Medicine, Tokyo, Japan
- <sup>5</sup> Department of Physiology, Keio University School of Medicine, Tokyo, Japan
- <sup>6</sup> Department of Neuropsychiatry, Keio University School of Medicine, Tokyo, Japan

## Abbreviations

CPR	Caudate-to-putamen ratio
DAT	Dopamine transporter
DLB	Dementia with Lewy bodies
FEW	Family-wise error
LB	Lewy body
LBD	Lewy body diseases
MMSE	Mini-mental state examination
PCR	Putamen-to-caudate ratio
PD	Parkinson's disease
PDD	Parkinson's disease with dementia
SBR	Specific binding ratio
SPECT	Single-photon emission computed tomography
SPM	Statistical parametric mapping
3D-SSP	Three-dimensional stereotactic surface projection
VOI	Volume of interest

## Introduction

Lewy body diseases (LBD), which are sequential neurodegenerative disorders and have many common clinical features and neuropathology, are considered subtypes of an  $\alpha$ -synuclein-associated disease spectrum from incidental LBD and non-demented Parkinson's disease (PD) to PD with dementia (PDD) and dementia with Lewy bodies (DLB). Although the nosologic relationship among these disorders is frequently being debated, it is currently difficult to classify them explicitly. Based on the conventional international consensus, DLB is diagnosed when cognitive impairment precedes parkinsonian motor symptoms or begins 1 year after the onset of parkinsonian; in contrast, in PDD, cognitive impairment develops in the setting of well-established PD [1]. Therefore, the diagnosis of LBD depends on the presence and timing of onset of cognitive impairment. Braak et al. proposed that LB pathology spreads via the olfactory bulb or gastrointestinal system from the peripheral to central nervous systems, and LB travels from the brainstem to the cortex [2]. The distribution and degree of LB pathology in the brain affect clinical symptoms in patients with LBD, including movement disorder, psychotic state, visual hallucination, and cognitive impairment, in patients with LBD.

Nuclear medicine imaging is useful in diagnosing LBD. Brain perfusion single-photon emission computed tomography (SPECT) shows changes in brain perfusion in this patient group. Notably, patients with PDD and DLB show parietal, temporal, or occipital hypoperfusion, while those with PD show no remarkable deterioration in brain perfusion compared with those with PDD or DLB [3]. These changes are related to cognitive impairment in these patients [4]. In addition, dopamine transporter (DAT)-SPECT is another useful nuclear medicine imaging approach to assess the function of the presynaptic nigrostriatal dopaminergic system. Quantitative indices calculated from DAT-SPECT are also useful in interpreting and assessing images [5, 6]. In patients with LBD, striatal tracer accumulation deteriorates as the disease condition progresses [7, 8]. The specific binding ratio (SBR), representing the strength of striatal tracer accumulation, is the most frequently used quantitative index in DAT-SPECT. Although the SBR index is useful because it correlates with the severity of motor dysfunction in patients with PD [9], it is not enough to differentiate between patients with PD and DLB [10]. On the other hand, the putamen-to-caudate (PCR) and caudate-to-putamen (CPR) ratios are different types of quantitative indices of DAT-SPECT that represent changes in the shape and distribution of striatal tracer accumulation. Accumulating studies have demonstrated that the PCR/CPR indices can differentiate patients

with PD and DLB [10–12]. It is speculated that the anterior part of striatal uptake, especially caudate uptake, correlates with psychotic state or cognitive impairment, while the posterior part of striatal uptake correlates with movement disorders in patients with LBD.

We hypothesised that changes in striatal tracer accumulation on DAT-SPECT would correlate with brain perfusion in patients with LBD and that these changes would reflect their symptoms, such as movement disorder or cognitive impairment, caused by differential distributions of LB pathology in the brain. Accordingly, this study aimed to assess the correlation between brain perfusion and quantitative indices (SBR, PCR, and CPR indices) of DAT-SPECT using the statistical parametric mapping (SPM) analysis and to compare these quantitative indices among patients with LBD, including PD, PDD, and DLB.

## Materials and Methods

### Patients

A total of 231 consecutive patients who underwent brain perfusion SPECT with N-isopropyl-p-[ $^{123}\text{I}$ ] iodoamphetamine (IMP) and DAT-SPECT with  $^{123}\text{I}$ -ioflupane from February 2014 to January 2019 were included in this retrospective study. The interval between the two examinations was less than 1 year. Patients with a disease that affects the image quality of DAT and brain perfusion SPECT (e.g., extensive cerebral haemorrhage and infarction) were excluded. Enrolled patients were diagnosed based on the clinical diagnostic criteria of the UK Parkinson's Disease Society Brain Bank [13] or established diagnostic criteria [1, 14]. Patients who were clinically undiagnosed with LBD were also excluded. General cognitive function was assessed in some of the participants using the mini-mental state examination (MMSE). Of the total 231 patients, 135 overlapped with those in our previous studies [10, 15].

The institutional review board of Keio University School of Medicine granted permission for this retrospective review of clinical data and imaging and waived the requirement for obtaining informed consent from the patients (approval number: 20211068).

### Image Acquisition and Reconstruction

Fifteen minutes after injection of 222 MBq of  $^{123}\text{I}$ -IMP, brain perfusion SPECT were obtained on Discovery NM 630 or Discovery NM/CT 670 (GE Healthcare, Milwaukee, WI) equipped with an extended low-energy general-purpose collimator. Projection data were acquired for 30 min. Imaging parameters were as follows: matrix size,  $128 \times 128$ ; pixel size, 2.9 mm; slice thickness, 2.9 mm; and energy window,

159 keV  $\pm$  10%. Data were reconstructed by the filtered back-projection method with a Butterworth filter (critical frequency, 0.45; power, 10.0). Attenuation correction was used, while scatter correction was not.

Three hours after injection of 185 MBq  $^{123}\text{I}$ -ioflupane, DAT-SPECT were obtained on the Discovery NM 630 or Discovery NM/CT 670 (GE Healthcare, Milwaukee, WI) equipped with a FAN beam collimator. Projection data were acquired for 30 min. Imaging parameters were as follows: matrix size, 128  $\times$  128; pixel size, 4.4 mm; slice thickness, 4.4 mm; and energy window, 159 keV  $\pm$  10%. Data were reconstructed by the ordered-subset expectation–maximisation method (iterations, 3; subset, 10) with a Butterworth filter (critical frequency, 0.5; power, 10.0). Neither attenuation correction nor scatter correction was used.

### Image Analysis of DAT-SPECT

We used commercially available software—DaTQUANT (GE Healthcare, Little Chalfont, UK) for calculation of quantitative indices of DAT-SPECT. DaTQUANT applies a normalised volume of interest (VOI) template, two striatal VOIs and two occipital lobe VOIs, based on the large European multi-centre database of healthy controls (ENC-DAT trial) (Fig. 2) [16, 17]. DaTQUANT enables setting these normalised VOIs automatically and calculation of the different types of quantitative indices: the SBR and PCR [10, 15, 18]. The SBR is defined as the mean counts of the striatal VOI (background-subtracted) divided by the mean counts of the occipital lobe VOI. The PCR is defined as the mean counts of the putamen VOI divided by the mean counts of the caudate VOI. We also calculated the CPR index, which is defined as the mean counts of the caudate VOI divided by the mean counts of the putamen VOI, as the simple reciprocal of the PCR index. In this study, the average values of the SBR and PCR/CPR for both sides of the striatum were used for the analysis.

### Statistical Model

The Kruskal–Wallis test was used to compare age, quantitative indices (SBR, PCR, and CPR), and the MMSE between the LBD (PD, PDD, and DLB) groups. If there were significant differences, post hoc analysis with Bonferroni correction was performed. The Pearson's chi-square test was used to compare sex between these groups. These tests were performed using SPSS software (version 27; SPSS Inc., Chicago, IL).

Brain perfusion imaging data were preprocessed and analysed with statistical parametric mapping (SPM) software (<https://www.fil.ion.ucl.ac.uk/spm/software/spm12/>), running on the Matlab R2020a software environment (MathWorks, Natick, MA). Brain perfusion SPECT data were first

aligned and anatomically standardised to match each scan to the Montreal Neurological Institute (MNI) atlas based template (McGill University, Montreal, Canada) using a 12-parameter affine transformation, followed by non-linear transformations [19, 20]. SPECT images were then smoothed with an 8  $\times$  8  $\times$  8 mm Gaussian filter. Normalisation of global brain counts to a value of 50 was performed with proportional scaling to remove differences in global activity in and between subjects. Proportional scaling was performed by dividing each voxel value by the average value of the whole parenchyma [21, 22]. Linear regression analyses after adjusting for age were conducted to determine the correlations between brain perfusion and quantitative indices calculated from DAT-SPECT and between brain perfusion and MMSE scores.

The initial voxel threshold was set to 0.001 uncorrected for multiple comparisons. Clusters were considered significant when falling below a cluster-corrected  $p$  (family-wise error [FWE]) = 0.05. If statistical significance was not reached, the threshold at the voxel level was explored at  $p < 0.001$  uncorrected.

## Results

Of the included 231 consecutive patients, four were excluded from the study due to insufficient image quality because of extensive cerebral haemorrhage and infarction, along with 192 who were clinically undiagnosed with LBD. The remaining 35 patients (median age, 76.0 years; range, 58–91 years; men/women, 13/22), including eight with PD, three with PDD, and 24 with DLB, were included in this analysis. Figure 1 depicts the flow diagram of study participants.

Table 1 shows the characteristics of included patients. The means and standard deviations of the SBR, PCR, and CPR indices and MMSE scores are also shown. Significant differences were observed in age, and the PCR and CPR indices between the PD and DLB groups.

Figure 2 shows representative images of DAT-SPECT and brain perfusion SPECT in patients with PD and DLB, and the calculated quantitative indices are also shown. PD cases tended to have lower PCR values, while DLB cases tended to have lower CPR values.

Figures 3, 4, and 5 show the results of the SPM analysis. The PCR/CPR indices showed significant correlations with brain perfusion (Figs. 3 and 4), while no significant correlation was observed between the SBR index and brain perfusion (data not shown). Decreased PCR index correlated with hypoperfusion in the brainstem (medulla oblongata and midbrain) (uncorrected  $p < 0.001$ ,  $k > 100$ ; Fig. 3), and decreased CPR index correlated with hypoperfusion in the right temporoparietal cortex (FWE corrected

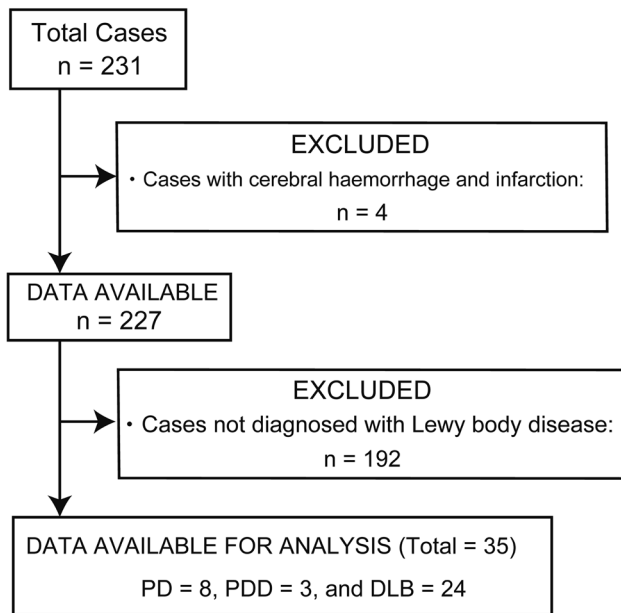


**Fig. 1** Flow diagram of patient inclusion. DLB, dementia with Lewy body; PD, Parkinson's disease; PDD, Parkinson's disease with dementia

**Table 1** Patient characteristics

Characteristics	PD	PDD	DLB
n	8	3	24
Age (years, mean $\pm$ SD)	67.1 $\pm$ 5.9*	80.3 $\pm$ 1.5	78.5 $\pm$ 6.6*
Sex (male/female)	2/6	1/2	10/14
Quantitative indices from DAT-SPECT			
SBR	1.18 $\pm$ 0.50	1.07 $\pm$ 0.86	1.09 $\pm$ 0.44
PCR	0.73 $\pm$ 0.08*	0.89 $\pm$ 0.16	0.89 $\pm$ 0.12*
CPR	1.38 $\pm$ 0.14*	1.15 $\pm$ 0.22	1.15 $\pm$ 0.16*
MMSE (n)	27.0 $\pm$ 2.8 (2)	24.0 $\pm$ 1.0 (3)	21.8 $\pm$ 5.5 (14)

CPR, caudate-to-putamen ratio; DAT, dopamine transporter; DLB, dementia with Lewy body; MMSE, mini-mental state examination; PCR, putamen-to-caudate ratio; PD, Parkinson's disease; PDD, Parkinson's disease with dementia; SBR, specific binding ratio; SD, standard deviation; SPECT, single-photon emission computed tomography

\*  $p < 0.05$  PD vs. DLB

$p < 0.05$ ), right precuneus (uncorrected  $p < 0.001$ ,  $k > 100$ ), and bilateral temporal cortex (uncorrected  $p < 0.001$ ,  $k > 100$ ; Fig. 4). A slight correlation between the MMSE score and brain perfusion was observed in the left temporoparietal cortex (uncorrected  $p < 0.001$ ; Fig. 5). Table 2 depicts the brain regions showing a significant correlation with the PCR/CPR indices.

## Discussion

This study showed that decreased putaminal uptake of  $^{123}\text{I}$ -ioflupane in DAT-SPECT significantly correlated with hypoperfusion in the brainstem; this correlation may reflect movement disorders in patients with LBD. Hacker et al. also demonstrated that midbrain-striatum functional connectivity was reduced in patients with PD, and in their study, striatal functional connectivity with the brainstem was graded as follows: posterior putamen  $>$  anterior putamen  $>$  caudate [23]. In addition, previous studies have shown more severe substantia nigra cell loss in PDD than in DLB, which consequently leads to more advanced parkinsonism [24]. The Hoehn and Yahr stage or Unified PD rating scale (motor part only) score has been reported to correlate with putaminal uptake of  $^{123}\text{I}$ -ioflupane in patients with PD [12]. These findings indicate that the midbrain-putamen dopaminergic connectivity contributes to motor dysfunction in patients with LBD. Thus, these findings represent a possibility that decreased PCR index could indicate enhanced severity of movement disorders caused by dysfunction of the putamen dopaminergic system connected from the brainstem.

We also demonstrated that decreased caudate uptake of  $^{123}\text{I}$ -ioflupane in DAT-SPECT was significantly correlated with hypoperfusion in the right temporoparietal cortex, right precuneus, and bilateral temporal lobes. Consistently, previous studies have shown that glucose hypometabolism in the temporoparietal areas correlates with dementia severity in LBD [25, 26] and that the caudate uptake of  $^{123}\text{I}$ -ioflupane correlates with cognitive impairment [25–30]. Our results and these previous findings indicate that the correlation between decreased CPR index and hypoperfusion in the temporoparietal cortex may reflect cognitive impairment in patients with LBD. In particular, a remarkable correlation (FWE corrected  $p < 0.05$ ) was observed between decreased CPR index and hypoperfusion in the right temporoparietal region in patients with LBD. Patients with PD and DLB are more likely to have visuospatial dysfunction than those with Alzheimer's disease [31, 32], and previous studies have reported that visuospatial dysfunction presents as right-dominant hypoperfusion or hypometabolism in the brain [33–35]. In addition, Marquie et al. demonstrated that reduced caudate DAT concentration was associated with worse visuospatial ability in patients with DLB [36]. These findings indicate that significant hypoperfusion in the right temporoparietal region may be indicative of the visuospatial dysfunction observed in patients with LBD. Our results also showed that hypoperfusion in the precuneus is correlated with decreased caudal uptake of  $^{123}\text{I}$ -ioflupane on DAT-SPECT; however, the posterior cingulate was spared from this hypoperfusion.

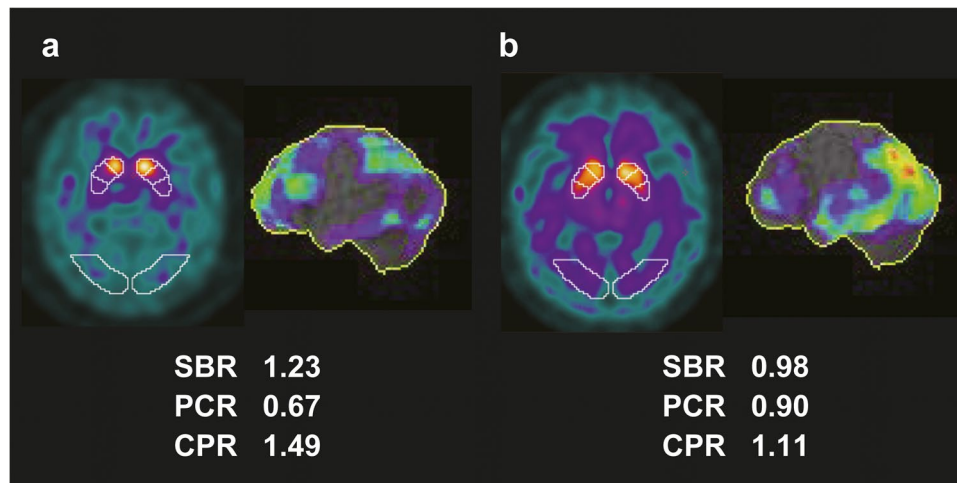


**Fig. 2** DAT-SPECT and brain perfusion SPECT images of representative cases of PD and DLB. A commercially available software package DaTQUANT was used for VOI-based analysis. The brain perfusion image was visualised with 3D-SSP. **a** A representative case of PD (aged 66 years, female) shows striatal uptake deterioration, especially in the posterior part. **b** A representative case of DLB

(aged 76 years, male) shows diffuse striatal uptake deterioration and remarkable hypoperfusion in the temporoparietal lobe. DAT, dopamine transporter; DLB, dementia with Lewy body; PD, Parkinson's disease; SPECT, single-photon emission computed tomography; VOI, volume of interest; 3D-SSP, three-dimensional stereotactic surface projection

This finding represents a characteristic sign, known as the “cingulate island sign,” observed on the brain perfusion SPECT of patients with DLB [37]. Early caudate dopaminergic dysfunction is reportedly also a predictor of future cognitive impairment [38–40]. Cognitive decline and related symptoms are not a consequence of  $\alpha$ -synuclein-induced neurodegeneration alone because amyloid  $\beta$  and tau pathologies also contribute to overall deficits [41–45]. These pathological changes may synergistically influence clinical features, including a shorter duration or a more malignant course [46, 47]. Therefore, we speculate that the CPR index has the potential to indicate the severity

of cognitive impairment and clinical course in patients with LBD.

This study found that the SBR index had no significant correlation with brain perfusion. This result suggests that, unlike the PCR/CPR indices, the SBR index, which represents the magnitude of striatal uptake of  $^{123}\text{I}$ -ioflupane, has little advantage for assessing the symptoms of motor/cognitive dysfunctions in patients with LBD.

We demonstrated that global cognitive impairment measured using the MMSE correlated with left temporoparietal cortex hypoperfusion in patients with LBD. Moreover, left-sided lateralisation has been observed between brain

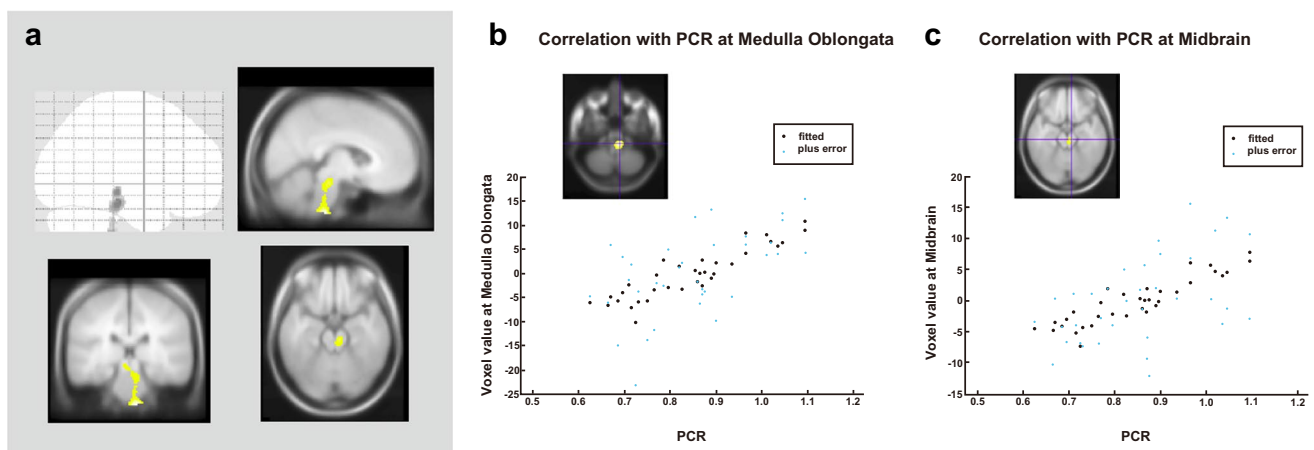


**Fig. 3** Correlations between brain perfusion SPECT and the PCR index. The PCR index correlated with brain hypoperfusion in the brain stem (medulla oblongata and midbrain) (uncorrected  $p < 0.001$ ,

$k > 100$  voxels). Regression lines at notable regions are shown. PCR, putamen-to-caudate ratio; SPECT, single-photon emission computed tomography

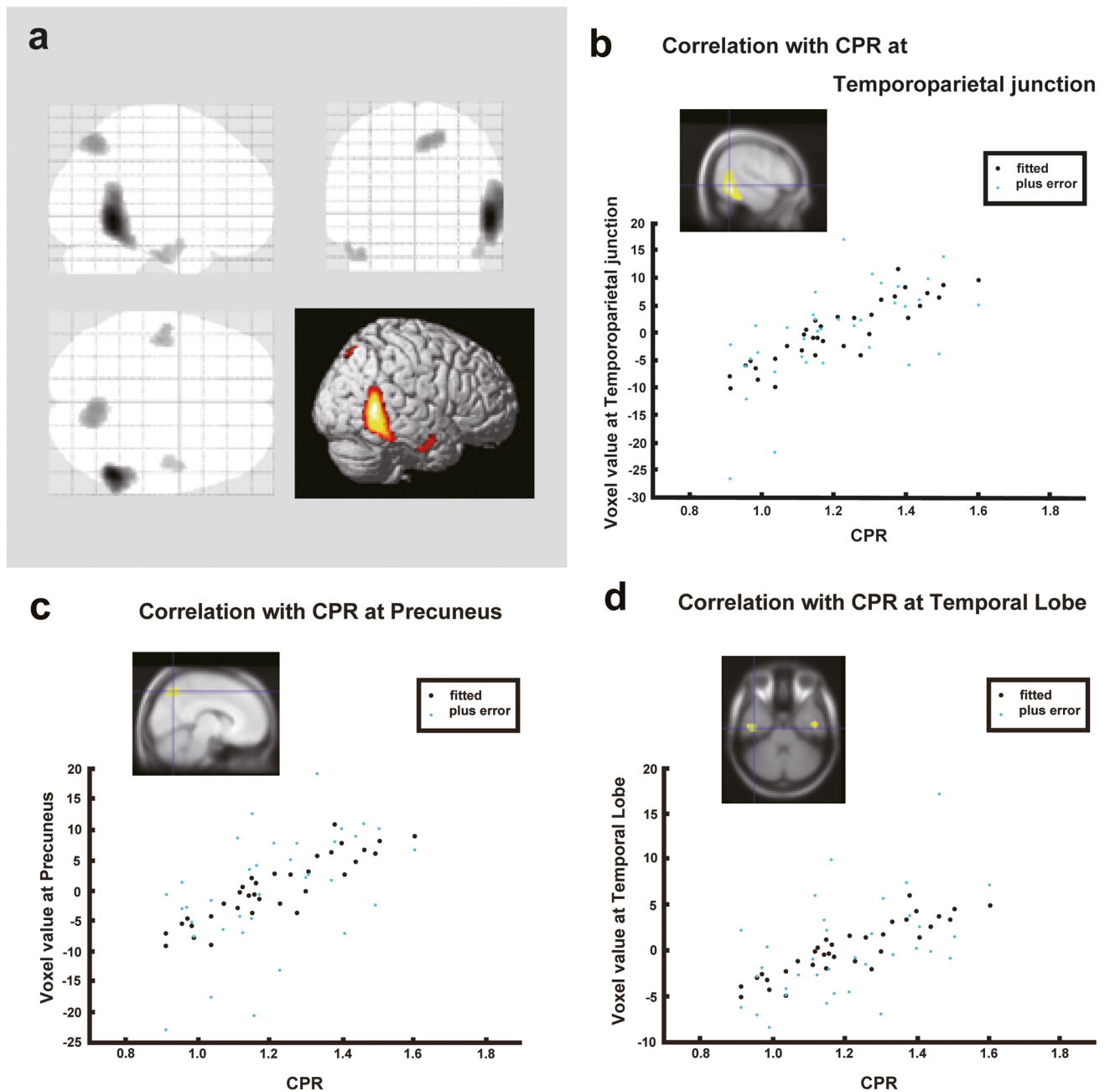


**Fig. 4** Correlations between brain perfusion SPECT and the CPR index. The CPR index correlated with brain hypoperfusion in the right temporoparietal cortex (FEW corrected  $p < 0.05$ ), right precuneus (uncorrected  $p < 0.001$ ,  $k > 100$  voxels), and bilateral temporal

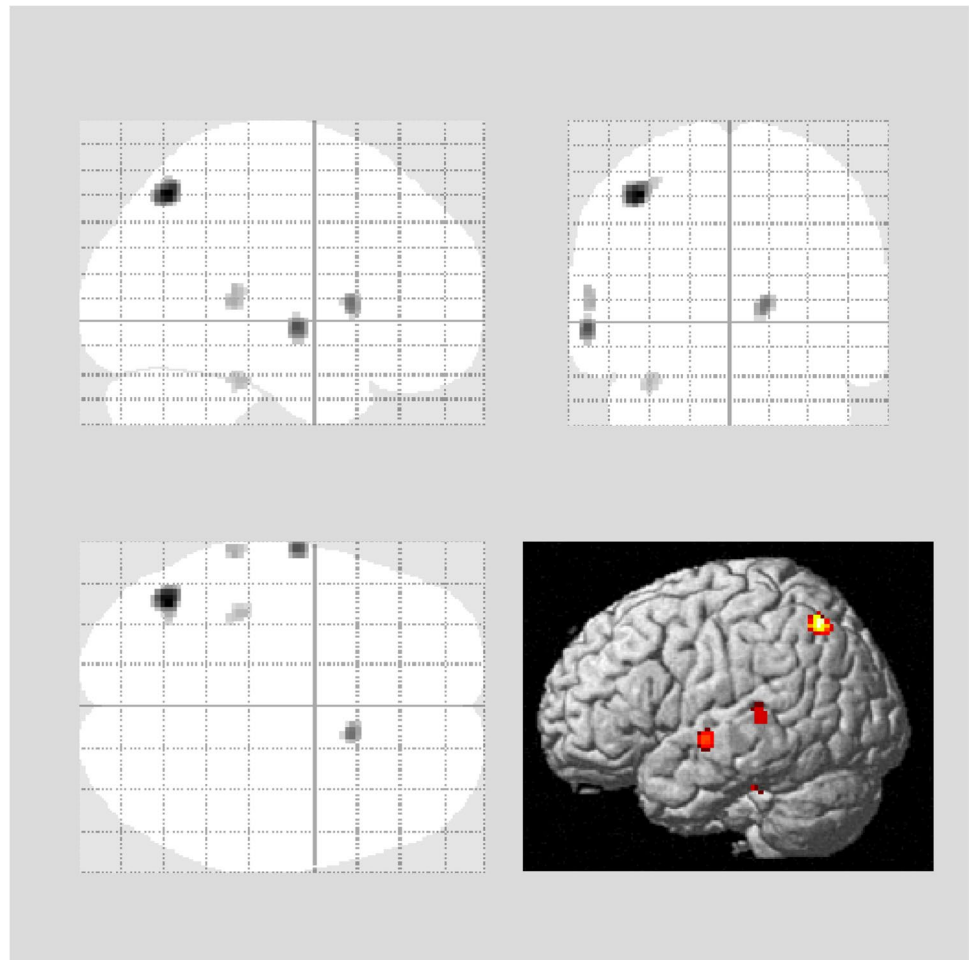
cortex (uncorrected  $p < 0.001$ ,  $k > 100$  voxels). Regression lines at notable regions are shown. CPR, caudate-to-putamen ratio; SPECT, single-photon emission computed tomography

perfusion and the MMSE score in patients with Alzheimer's disease [48, 49], probably because most of the items of the MMSE questionnaire rely on left hemispheric cognitive processing.

Some patients included in this study overlapped with those included in our previous studies [10, 15]. In our previous studies, we assessed the combined diagnostic utility of the quantitative indices of DAT-SPECT or

iodine-131-meta-iodobenzylguanidine scintigraphy for PD and atypical parkinsonian syndromes; however, we did not use brain perfusion SPECT or assess the correlation between brain perfusion and DAT-SPECT in LBD [10, 15]. Nobili et al. previously evaluated the correlation between brain perfusion and DAT-SPECT in patients with PD and found that brain perfusion in the posterior cingulate, parahippocampal gyrus, and middle temporal

**Fig. 5** Correlations between brain perfusion SPECT and the MMSE scores. The MMSE scores correlated with brain hypoperfusion in the left temporoparietal cortex (uncorrected  $p < 0.001$ ). Regression lines at notable regions are shown. MMSE, Mini-Mental State Examination; SPECT, single-photon emission computed tomography



gyrus correlated with uptake in the caudate, whereas that in the posterior cingulate, parietal precuneus, and occipital cuneus correlated with uptake in the putamen [50].

However, their study enrolled only patients with PD, and they used the SBR of the caudate/putamen regions, not the PCR or CPR, as quantitative indices. The PCR/CPR

**Table 2** Brain areas showing a significant correlation with the PCR and CPR indices

Area	Cluster size	Coordinates			Z-score	p values (uncorrected, $k > 100$ )
		X	Y	Z		
PCR						
Medulla oblongata	165	8	-30	-52	3.88	<0.001
Mid Bbrain	168	8	-24	-18	3.41	<0.001
CPR						
R temporoparietal lobe	1295	54	-54	-4	4.26	<0.05 (FWE corrected)
R precuneus	427	8	-66	50	3.52	<0.001
L temporal lobe	137	-42	-16	-32	3.41	<0.001
R temporal lobe	106	48	-10	-30	3.29	<0.001

CPR, caudate-to-putamen ratio; FWE, family-wise error; L, left; MMSE, mini-mental state examination; PCR, putamen-to-caudate ratio; R, right

indices have been suggested to be particularly valuable as they are background-, age-, and camera-independent [6]. These factors may explain the difference between our findings and theirs.

This study has some limitations. First, the number of patients analysed was relatively small. Additional studies with larger numbers of participants are needed to confirm our observations. Second, the diagnoses of PD, PDD, and DLB were clinical diagnoses and not pathologically confirmed. Finally, this was a single-centre study, and institution-specific factors might limit the generalizability of our results.

## Conclusion

This study found that changes in striatal tracer accumulation on DAT-SPECT correlated with brain hypoperfusion in several specific regions (brainstem, temporoparietal cortex, or precuneus) in patients with LBD.

**Acknowledgements** The authors thank the staff of the Division of Nuclear Medicine at the Department of Radiology for their valuable support.

**Author Contribution** YI, TS, and MJ were responsible for the design of the study; YI and RM collected the SPECT data; YI performed the statistical analysis; MS, DI, HU, and HT supported the selection of clinical data; and YI, TS, KM, MS, DI, HU, and HT drafted the manuscript. All authors read and critiqued the manuscript and approved the final version of the manuscript.

**Funding** This work was supported by JSPS KAKENHI (Grant Number: JP19K17243).

**Data Availability** All data generated or analysed during this study are included in this published article.

## Declarations

**Ethics Approval** This study was approved by the Ethics Committee of Keio University School of Medicine (registration number: 20211068). This article does not contain any data from experiments with animals performed by any of the authors. All procedures performed in this study involving human participants were in accordance with the ethical standards of the institutional and/or national research committee and with the 1964 Helsinki declaration and its later amendments or comparable ethical standards.

**Consent to Participate** The institutional review board of the hospital granted permission for this retrospective review of imaging and clinical data and waived the requirement for obtaining informed consent from the patients.

**Competing Interests** MJ received research grants from Nihon Medi-Physics Co., Ltd. and GE Healthcare Corp. MK received a research grant from Nihon Medi-Physics Co., Ltd. Other authors declare no conflict of interest.

**Open Access** This article is licensed under a Creative Commons Attribution 4.0 International License, which permits use, sharing, adaptation, distribution and reproduction in any medium or format, as long as you give appropriate credit to the original author(s) and the source, provide a link to the Creative Commons licence, and indicate if changes were made. The images or other third party material in this article are included in the article's Creative Commons licence, unless indicated otherwise in a credit line to the material. If material is not included in the article's Creative Commons licence and your intended use is not permitted by statutory regulation or exceeds the permitted use, you will need to obtain permission directly from the copyright holder. To view a copy of this licence, visit <http://creativecommons.org/licenses/by/4.0/>.

## References

1. Emre M, Aarsland D, Brown R et al (2007) Clinical diagnostic criteria for dementia associated with Parkinson's disease. *Mov Disord* 22:1689–1707
2. Braak H, Del Tredici K, Rüb U et al (2003) Staging of brain pathology related to sporadic Parkinson's disease. *Neurobiol Aging* 24:197–211
3. Mito Y, Yoshida K, Yabe I et al (2004) Brain 3D-SSP SPECT analysis in dementia with Lewy bodies, Parkinson's disease with and without dementia, and Alzheimer's disease. *Clin Neurol Neurosurg* 107:396–403
4. Jokinen P, Scheinin N, Aalto S et al (2010) [(11)C]PIB-, [(18)F]FDG-PET and MRI imaging in patients with Parkinson's disease with and without dementia. *Parkinsonism Relat Disord* 16:666–670
5. Roberts G, Kane JPM, Lloyd JJ et al (2019) A comparison of visual and semiquantitative analysis methods for planar cardiac 123I-MIBG scintigraphy in dementia with Lewy bodies. *Nucl Med Commun* 40:734–743
6. Söderlund TA, Dickson JC, Prvulovich E et al (2013) Value of semiquantitative analysis for clinical reporting of 123I-2- $\beta$ -carbomethoxy-3 $\beta$ -(4-iodophenyl)-N-(3-fluoropropyl)nortropane SPECT studies. *J Nucl Med* 54:714–722
7. Mito Y, Yabe I, Yaguchi H et al (2020) Relations of clinical symptoms with dopamine transporter imaging in drug-naïve Parkinson's disease. *Clin Neurol Neurosurg* 196:105960
8. Ravina B, Marek K, Eberly S et al (2012) Dopamine transporter imaging is associated with long-term outcomes in Parkinson's disease. *Mov Disord* 27:1392–1397
9. Kuribara T, Enatsu R, Kitagawa M et al (2020) Neuroimaging and neurophysiological evaluation of severity of Parkinson's disease. *J Clin Neurosci* 74:135–140
10. Iwabuchi Y, Kameyama M, Matsusaka Y et al (2021) A diagnostic strategy for Parkinsonian syndromes using quantitative indices of DAT SPECT and MIBG scintigraphy: an investigation using the classification and regression tree analysis. *Eur J Nucl Med Mol Imaging* 48:1833–1841
11. Joling M, Vriend C, van der Zande JJ et al (2018) Lower (123)I-FP-CIT binding to the striatal dopamine transporter, but not to the extrastriatal serotonin transporter, in Parkinson's disease compared with dementia with Lewy bodies. *Neuroimage Clin* 19:130–136
12. Walker Z, Costa DC, Walker RW et al (2004) Striatal dopamine transporter in dementia with Lewy bodies and Parkinson disease: a comparison. *Neurology* 62:1568–1572
13. Gibb WR, Lees AJ (1988) The relevance of the Lewy body to the pathogenesis of idiopathic Parkinson's disease. *J Neurol Neurosurg Psych* 51:745–752



14. McKeith IG, Boeve BF, Dickson DW et al (2017) Diagnosis and management of dementia with Lewy bodies: fourth consensus report of the DLB Consortium. *Neurology* 89:88–100
15. Iwabuchi Y, Nakahara T, Kameyama M et al (2019) Impact of a combination of quantitative indices representing uptake intensity, shape, and asymmetry in DAT SPECT using machine learning: comparison of different volume of interest settings. *EJNMMI Res* 9:7
16. Varrone A, Dickson JC, Tossici-Bolt L et al (2013) European multicentre database of healthy controls for [123I]FP-CIT SPECT (ENC-DAT): age-related effects, gender differences and evaluation of different methods of analysis. *Eur J Nucl Med Mol Imaging* 40:213–227
17. Brogley JE (2019) DaTQUANT: The future of diagnosing Parkinson disease. *J Nucl Med Technol* 47:21–26
18. Morbelli S, Arnaldi D, Cella E et al (2020) Striatal dopamine transporter SPECT quantification: head-to-head comparison between two three-dimensional automatic tools. *EJNMMI Res* 10:137
19. Friston KJ, Holmes AP, Worsley KJ et al (1995) Statistical parametric maps in functional imaging: a general linear approach. *Hum Brain Mapp* 2:189–210
20. Calhoun VD, Wager TD, Krishnan A et al (2017) The impact of T1 versus EPI spatial normalization templates for fMRI data analyses. *Hum Brain Mapp* 38:5331–5342
21. Stamatakis EA, Glabus MF, Wyper DJ et al (1999) Validation of statistical parametric mapping (SPM) in assessing cerebral lesions: a simulation study. *Neuroimage* 10:397–407
22. López-González FJ, Silva-Rodríguez J, Paredes-Pacheco J et al (2020) Intensity normalization methods in brain FDG-PET quantification. *Neuroimage* 222:117229
23. Hacker CD, Perlmutter JS, Criswell SR et al (2012) Resting state functional connectivity of the striatum in Parkinson's disease. *Brain* 135:3699–3711
24. Tsuboi Y, Dickson DW (2005) Dementia with Lewy bodies and Parkinson's disease with dementia: are they different? *Parkinsonism Relat Disord* 11(Suppl 1):S47-51
25. Schapiro MB, Pietrini P, Grady CL et al (1993) Reductions in parietal and temporal cerebral metabolic rates for glucose are not specific for Alzheimer's disease. *J Neurol Neurosurg Psychiatry* 56:859–864
26. Vander Borgh T, Minoshima S, Giordani B et al (1997) Cerebral metabolic differences in Parkinson's and Alzheimer's diseases matched for dementia severity. *J Nucl Med* 38:797–802
27. Ekman U, Eriksson J, Forsgren L et al (2012) Functional brain activity and presynaptic dopamine uptake in patients with Parkinson's disease and mild cognitive impairment: a cross-sectional study. *Lancet Neurol* 11:679–687
28. Müller U, Wächter T, Barthel H et al (2000) Striatal [123I]beta-CIT SPECT and prefrontal cognitive functions in Parkinson's disease. *J Neural Transm (Vienna)* 107:303–319
29. Nobili F, Campus C, Arnaldi D et al (2010) Cognitive-nigrostriatal relationships in de novo, drug-naïve Parkinson's disease patients: a [I-123]FP-CIT SPECT study. *Mov Disord* 25:35–43
30. Pellecchia MT, Picillo M, Santangelo G et al (2015) Cognitive performances and DAT imaging in early Parkinson's disease with mild cognitive impairment: a preliminary study. *Acta Neurol Scand* 131:275–281
31. Ferman TJ, Arvanitakis Z, Fujishiro H et al (2013) Pathology and temporal onset of visual hallucinations, misperceptions and family misidentification distinguishes dementia with Lewy bodies from Alzheimer's disease. *Parkinsonism Relat Disord* 19:227–231
32. Johnson DK, Morris JC, Galvin JE (2005) Verbal and visuospatial deficits in dementia with Lewy bodies. *Neurology* 65:1232–1238
33. Han JY, Byun MS, Seo EH et al (2015) Functional neural correlates of figure copy and recall task performances in cognitively impaired individuals: an 18F-FDG-PET study. *NeuroReport* 26:1077–1082
34. Melrose RJ, Harwood D, Khoo T et al (2013) Association between cerebral metabolism and Rey-Osterrieth complex figure test performance in Alzheimer's disease. *J Clin Exp Neuropsychol* 35:246–258
35. Tippet WJ, Black SE (2008) Regional cerebral blood flow correlates of visuospatial tasks in Alzheimer's disease. *J Int Neuropsychol Soc* 14:1034–1045
36. Marquie M, Locascio JJ, Rentz DM et al (2014) Striatal and extrastriatal dopamine transporter levels relate to cognition in Lewy body diseases: an (11)C altropane positron emission tomography study. *Alzheimers Res Ther* 6:52
37. Imabayashi E, Yokoyama K, Tsukamoto T et al (2016) The cingulate island sign within early Alzheimer's disease-specific hypoperfusion volumes of interest is useful for differentiating Alzheimer's disease from dementia with Lewy bodies. *EJNMMI Res* 6:67
38. Arnaldi D, Campus C, Ferrara M et al (2012) What predicts cognitive decline in de novo Parkinson's disease? *Neurobiol Aging* 33:1127.e11–20
39. Caspell-Garcia C, Simuni T, Tosun-Turgut D et al (2017) Multiple modality biomarker prediction of cognitive impairment in prospectively followed de novo Parkinson disease. *PLoS ONE* 12:e0175674
40. Schrag A, Siddiqui UF, Anastasiou Z et al (2017) Clinical variables and biomarkers in prediction of cognitive impairment in patients with newly diagnosed Parkinson's disease: a cohort study. *Lancet Neurol* 16:66–75
41. Colom-Cadena M, Gelpi E, Charif S et al (2013) Confluence of  $\alpha$ -synuclein, tau, and  $\beta$ -amyloid pathologies in dementia with Lewy bodies. *J Neuropathol Exp Neurol* 72:1203–1212
42. Colom-Cadena M, Grau-Rivera O, Planellas L et al (2017) Regional overlap of pathologies in Lewy body disorders. *J Neuropathol Exp Neurol* 76:216–224
43. Howlett DR, Whitfield D, Johnson M et al (2015) Regional multiple pathology scores are associated with cognitive decline in Lewy body dementias. *Brain Pathol* 25:401–408
44. Kapasi A, DeCarli C, Schneider JA (2017) Impact of multiple pathologies on the threshold for clinically overt dementia. *Acta Neuropathol* 134:171–186
45. Walker L, McAleese KE, Thomas AJ et al (2015) Neuropathologically mixed Alzheimer's and Lewy body disease: burden of pathological protein aggregates differs between clinical phenotypes. *Acta Neuropathol* 129:729–748
46. Ferman TJ, Aoki N, Crook JE et al (2018) The limbic and neocortical contribution of  $\alpha$ -synuclein, tau, and amyloid  $\beta$  to disease duration in dementia with Lewy bodies. *Alzheimers Dement* 14:330–339
47. Irwin DJ, Grossman M, Weintraub D et al (2017) Neuropathological and genetic correlates of survival and dementia onset in synucleinopathies: a retrospective analysis. *Lancet Neurol* 16:55–65
48. Apostolova LG, Lu PH, Rogers S et al (2006) 3D mapping of mini-mental state examination performance in clinical and preclinical Alzheimer disease. *Alzheimer Dis Assoc Disord* 20:224–231
49. Lampl Y, Sadeh M, Laker O et al (2003) Correlation of neuropsychological evaluation and SPECT imaging in patients with Alzheimer's disease. *Int J Geriatr Psychiatry* 18:288–291
50. Nobili F, Arnaldi D, Campus C et al (2011) Brain perfusion correlates of cognitive and nigrostriatal functions in de novo Parkinson's disease. *Eur J Nucl Med Mol Imaging* 38:2209–2218